GU J Sci, Part A, 8(2): 299-307 (2021)

Gazi University

Journal of Science

PART A: ENGINEERING AND INNOVATION

http://dergipark.gov.tr/gujsa

Araştırma Makalesi Research Article

Effect of Post-Annealing Treatment on the Structural, Optical, and Electrical Properties of V_2O_5 Thin Films

Semih INCECAM[1,2*], Adem SARAC[1,2], Evren ERDIL[1,2], Ali Orkun CAGIRTEKIN[3], Selim ACAR[2,3]

[1]*METU MEMS Center, Ankara, Turkey*
[2]*Department of Advanced Technologies, Graduate School of Natural and Applied Sciences, Gazi University, Ankara, Turkey*
[3]*Department of Physics, Science Faculty, Gazi University, Ankara, Turkey*

Keywords

Amorphous V_2O_5
Post-Annealing
DC Magnetron Sputtering
Thin Films
Characterization

Abstract

Vanadium pentoxide (V_2O_5) thin films were prepared on microscope glass slides using the reactive DC magnetron sputtering technique at room temperature. Post annealing process was performed at atmospheric conditions in 480°C for 1 hour. To investigate the effect of post-annealing treatment, morphological and structural analyses were carried out by field emission scanning electron microscopy (FESEM) and X-ray diffraction (XRD), respectively. Additionally optical characterization was completed using UV-Vis spectrophotometer. Current-voltage (I-V) and capacitance-voltage (C-V) measurements were performed to examine electrical properties. XRD revealed the drastic effect of post-annealing on the crystallization of amorphous V_2O_5 thin films. The amorphous as-deposited film structure transformed into the polycrystalline form after post-annealing treatment. FESEM images revealed a remarkable change in surface morphology from a smooth flat surface to a rough surface with the formation of V_2O_5 nanorods under the influence of post-annealing. Optical energy band gap was observed to decrease drastically. The significant changes in the structure and morphology of the thin films with post-annealing affected their electrical properties to a fair extent. While resistance increased, capacitance and dielectric permittivity of the films decreased with post-annealing treatment.

Cite

İnceçam, S., Saraç, A., Erdil, E., Çağırtekin, A. O., & Acar, S. (2021). Effect of post-annealing treatment on the structural, optical, and electrical properties of V_2O_5 thin films. *GU J Sci, Part A*, *8*(2), 299-307.

Author ID (ORCID Number)

S. İnceçam, 0000-0003-0417-3761
A. Saraç, 0000-0002-9099-4883
E. Erdil, 0000-0001-5079-8530
A.O. Çağırtekin, 0000-0001-8602-6233
S. Acar, 0000-0003-4014-7800

Article Process

Submission Date	30.04.2021
Revision Date	18.06.2021
Accepted Date	22.06.2021
Published Date	24.06.2021

1. INTRODUCTION

Vanadium oxides have received a lot of attention recently because of their complex stages within the vanadium-oxygen graph. Especially, vanadium pentoxide (V_2O_5), which is recently broadly utilized in electrical switching, catalysts, gas sensing, optoelectronic and smart thermochromic applications, has gotten major attention in research and innovation over the years among other MOS materials (Yan et al., 2015). Among different vanadium oxides, four compounds (namely VO, V_2O_3, VO_2, and V_2O_5) correspond to the single valence state of vanadium (that is, V^{2+}, V^{3+}, V^{4+} and V^{5+}, respectively). Due to their extraordinary basic adaptability as well as their extraordinary chemical and physical features that are essential in catalytic and electrochemical implementations, these oxides merit special attention (Hébert et al., 2002). V_2O_5 is a semiconductor oxide of n-type conductivity that can be affected by the change in the density of oxygen vacancies following any $V^{5+} \leftrightarrow V^{4+}$ transformation (Shimizu et al., 2009). Vanadium oxidation states rely on surrounding circumstances and production strategies. Nanostructured thin films can be synthesized by different techniques; like, sputtering (Cho et al., 2006; Xue-Jin et al., 2008; Ba et al., 2013; Luo et al., 2014), chemical vapor deposition (Kim et al., 1993; Kiri et al., 2011), sol-gel (Béteille & Livage, 1998; Wang et al., 2013), and

*Corresponding Author, e-mail: sincecam@mems.metu.edu.tr

pulsed laser deposition (Bowman & Gregg, 1998; Kumar et al., 2004). Various changes occurred in the structural and electrical properties of amorphous V_2O_5 by the post-annealing process. In similar studies in the literature, Zou et al. (2009; 2010) and Prześniak-Welenc et al. (2015) reported the effect of post-annealing on V_2O_5 thin films synthesized by different techniques. They found that after increasing the temperature up to 450-500°C, peaks appeared in XRD patterns. Besides that, samples that were post-annealed at 450°C and 500°C showed very thin V_2O_5 nanorods grown from the surface of the as-prepared V_2O_5 amorph film similar to Zou et al. (2010). After annealing at 500°C and higher temperatures, the V_2O_5 nanorods became larger (Zou et al., 2009) and thus 480°C has been chosen as the post-annealing temperature.

In this work, vanadium pentaoxide thin films were synthesized by the reactive DC magnetron sputtering method and then prepared by post-annealing in atmospheric conditions. The aim was to examine in detail the possible effects of post-annealing on the structural, optical and electrical properties of vanadium oxide thin films. For this purpose, unannealed and 480°C annealed samples were compared according to various measurements.

2. MATERIAL AND METHOD

The microscopy glass slides were used as substrates. Before vanadium oxide thin film was grown, the substrates were chemically cleaned to remove organic and other dirt on the surface. Ultrasonic cleaning were carried out in acetone for 10 minutes, isopropanol for 10 minutes and dried using nitrogen gas, sequentially. A series of amorphous V_2O_5 thin films were deposited on microscope glass slides at room temperature using AJA ATC Orion 3 sputter system with a base pressure 3×10^{-7} Torr. Amorphous V_2O_5 thin films were deposited by using a circular vanadium target of 4 inches (Kurt J. Lesker Co.) with a purity of 99.99%. Before the deposition process, to prevent surface contamination, the vanadium target was sputtered with Ar plasma for 3 minutes. The sputter parameters for amorphous V_2O_5 thin films are shown in Table 1. During deposition, without any heating, the substrates were placed on a rotating fixture which rotates at a speed of 80 rpm. The deposition time was 20 minutes, and the film thickness was approximately 210 nm which was measured by a step profilometer (Dektak, Bruker).

Table 1. *Sputtering Parameters for Amorphous V_2O_5 Thin Films*

Base Pressure	3×10^{-7} Torr
Sputtering Pressure	1.8 mTorr
Target	99.99% V
DC Power	550W
Sputtering gas	Pure Argon
$Ar:O_2$	30:4
Substrate Temperature	RT
Thickness	210 nm
Sputtering time	20 min

After deposition, the post-annealing was performed at 480ºC for 1 hour in the air. Throughout the paper, the as-grown (unannealed) and the 480°C annealed samples will be denoted respectively as AG and AT-480.

The phase structure of the synthesized thin films was identified by GI- X-ray diffraction (GIXRD, Rigaku, Ultima IV, Cu Kα emission), and their surface morphology was investigated by a field emission scanning electron microscopy (FESEM, Hitachi SU-8230). Besides, the samples' optical properties were investigated by a UV-Vis spectrophotometer (Shimadzu UV-1800). An uncoated microscope glass slide was used as a reference and the optical energy band gap of the thin films was calculated.

A pair of interdigitated Ni-Cr electrodes were deposited on the substrates with a shadow mask by DC magnetron sputtering. The sputter parameters for Ni-Cr IDT are shown in Table 2.

Table 2. *Sputtering Parameters for Ni-Cr IDT Electrodes*

Base Pressure	2×10^{-7} Torr
Sputtering Pressure	2.7 mTorr
Target	99.99% Ni/Cr (80/20wt%)
DC Power	100W
Sputtering gas	Pure Argon
$Ar:O_2$	30:0
Substrate Temperature	RT
Thickness	120 nm
Sputtering time	40 min

Electrical characterization of AG and AT-480 was investigated by a Keysight E4990A impedance analyzer and a Keithley 2400 source meter. The capacitance and conductance spectra of the AG and AT-480 samples were recorded in the frequency range from 1 kHz to 1.5 MHz. In addition to that current voltage measurements were performed.

3. RESULTS AND DISCUSSION

3.1. Structural and Morphological Characterizations

Structural properties of the thin films were probed by GIXRD technique and the corresponding patterns of the produced films are given in Figure 1. Clearly, AT-480 thin film showed a polycrystalline V_2O_5 structure with preferred (010) orientation while AG thin film showed an amorphous phase. This demonstrates the critical impact of post annealing on the structure of V_2O_5 thin films.

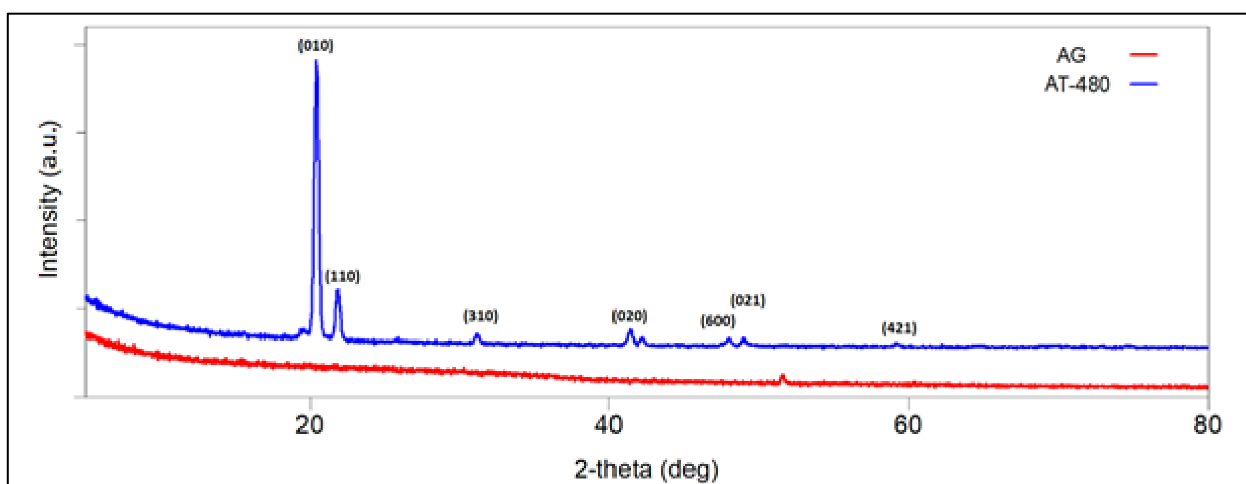

Figure 1. *GIXRD Patterns for AG and AT-480 V_2O_5 Thin Films*

In the XRD pattern, no obvious Bragg peaks were observed in the AG sample which corresponds to amorphous V_2O_5 material. However, the post-annealed sample AT-480 can be indexed to the orthorhombic V_2O_5 phase (ICDD: 01-72-0598). The sharpest peak appeared to indicate the V_2O_5 (010). This crystalline structure is the same as that reported for V_2O_5 nanorods by other research groups (Zou et al., 2009; Yan et al., 2015; Van de

Kerckhove et al., 2017). The crystalline property and grain size of the films were found to increase after annealing.

Surface morphologies of the synthesized films were examined through FESEM. To investigate the effect of post-annealing on the material, FE-SEM images in Figure 2 were taken from AT-480 and AG samples. The secondary electron (SE) detector of the device was used while these images were taken.

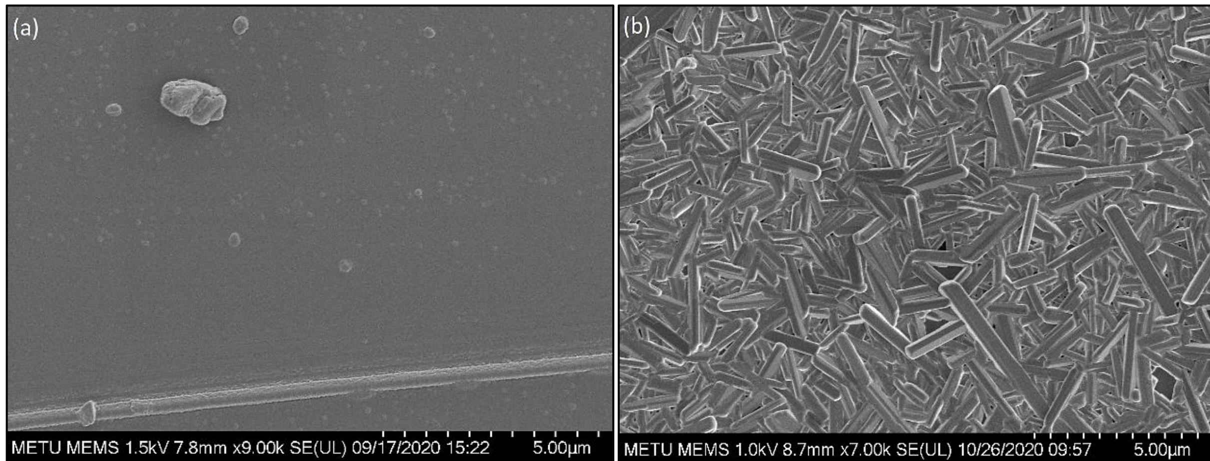

Figure 2. *FESEM Images of **a)** AG and **b)** AT-480 V_2O_5 Thin Films*

Structural differences are seen in Figure 2a and 2b. In Figure 2a of the AG sample, vanadium oxide is seen as a flat film. No nanostructural formation was observed on the surface. In Figure 2b, AT-480 thin film took the form of a nanorod by the post-annealing effect. The resulting nanorods have a 150-300 nm width and approximately a 1um length. This shows the impact of thermodynamic-based surface diffusions in the growth mechanism of nanorods (Zou et al., 2010). In a similar study in the literature, similar structures were observed in the SEM image taken from the vanadium oxide thin films, produced by Zou et al. (2009) with the sputtering technique.

3.2. Optical Characterization

The optical properties of thin films were examined by a UV-Vis spectrophotometer. Measurements were taken for AG and AT-480 samples in the 300-1100 nm wavelength range with the Shimadzu UV-1800 instrument. Using these, the Tauc graphs in Figure 3 were drawn with calculations and the energy bandgap range was calculated for each sample. The effect of post-annealing was investigated.

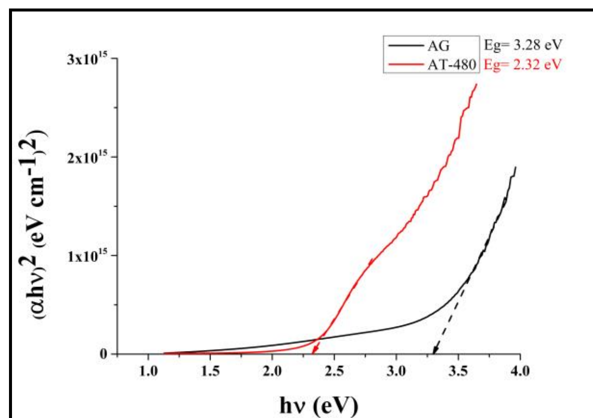

Figure 3. *$(\alpha h\upsilon)^2$ - hυ Graphs for AG and AT-480 V_2O_5 Thin Films*

The direct optical band gap (E_g) of the V_2O_5 films was estimated by extrapolating the linear region of $(\alpha h\upsilon)^2$ versus hυ curve to zero (Figure 3). From the $(\alpha h\upsilon)^2$ - hυ graph shown in Figure 3, the point where the slope of

the edge-tail intersects on the energy axis gives the optical energy band gap range for that material. The values of E_g were estimated as 3.28 eV and 2.32 eV for AG and AT-480 thin films, respectively.

Optical energy band gap was observed to decrease drastically. Indeed, upon exposure of the films to higher annealing temperatures in another literature study, a shift of the band gap to low energy was recorded implying that Vanadium oxides' band gaps decrease with the increase in annealing temperature (Yelsani et al., 2019). For the annealed V_2O_5 thin film, the optical energy band gap value was found similarly by Lamsal & Ravindra (2013) and Vijayakumar et al. (2014).

Similar observations were also reported in V_2O_5 films deposited by dip-coating technique (Vasanth Raj et al., 2013), it can also be explained by the quantum size effect in which the films have large size crystallites. However, the bandgap of V_2O_5 is dependent on the experimental conditions and preparation methods (Benmoussa et al., 2002; Rajendra Kumar et al., 2003).

3.3. Electrical Characterization

3.3.1. Current-Voltage

Current-voltage measurements were performed at room temperature to determine the effect of post-annealing on the resistance of the films. The current-voltage characteristic plot and corresponding resistances are displayed in Figure 4.

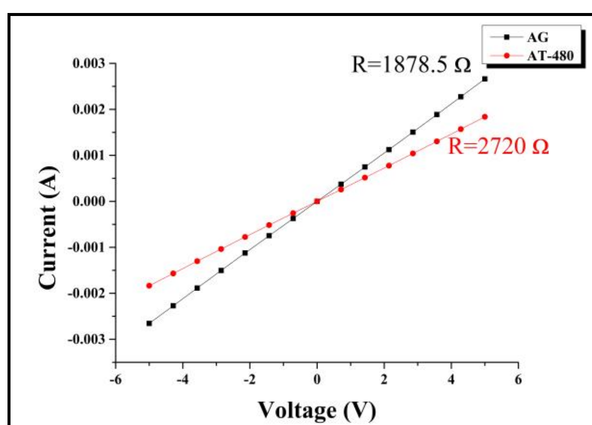

Figure 4. *Current-Voltage Curves for AG and AT-480 V_2O_5 Thin Films*

Obviously, surface resistance increased from 1878.5 Ω to 2720 Ω with the annealing process. This points out that electrical properties can change drastically with the annealing process. It is established that resistivity of a material is associated with carrier concentration and mobility (Hu et al., 2004). This behavior which is observed in some oxides such as ITO (Mohamed, 2007) and V_2O_5 (Mohamed, 2009) may be attributed to the process of oxygen chemisorption on the surface of the films where it behaves like an electron acceptor. The electrical resistivity increments slightly which may be due to the increment in the surface roughness as was seen by SEM images (Figure 2), due to the possible interaction of glass substrate and the produced films at high temperatures (Ramana et al., 2004; Mohamed, 2007).

3.3.2. Capacitance and Conductance

The capacitance and conductance measurements were performed over a frequency range of 1 kHz-1.5 MHz at room temperature. Figures 5a and 5b show respectively the capacitance-frequency and conductance-frequency measurements of both samples.

As can be seen from Figure 5a, the capacitance decreases with increasing frequency. Such a decrease can be best attributed to the inability of electric dipoles to follow the polarity of the high-frequency electric field and to the immobilization of charge carriers captured at deep traps (Budaguan et al., 1998). It can be also correlated with the confinement of charge carriers by gap states present more densely in amorph structures (Sengodan et al., 2013), and this explains the observed steep decrease in amorphous AG films and the gradual decrease in

AT 480 well-crystallized films. The AT-480 thin film showed nanorods and porous morphology of the surface as mentioned above. This can be the reason for the decrease of the capacitance of the V_2O_5 film after annealing at 480°C. As a result, a small number of charges were stored in V_2O_5 nanorods which gave down to its capacitance value.

As can be seen from Figure 5b, the measured conductance values increase with increasing frequencies. The conductance of both samples revealed similar behavior as a function of frequency. However, the effect of frequency on conductance was more prominent in AG samples than in AT 480 samples where the latter recorded a very slight increase in conductance with frequency as compared to the former. The conductance decreased slightly with the annealing process and this result is in line with the resistance result which was discussed above.

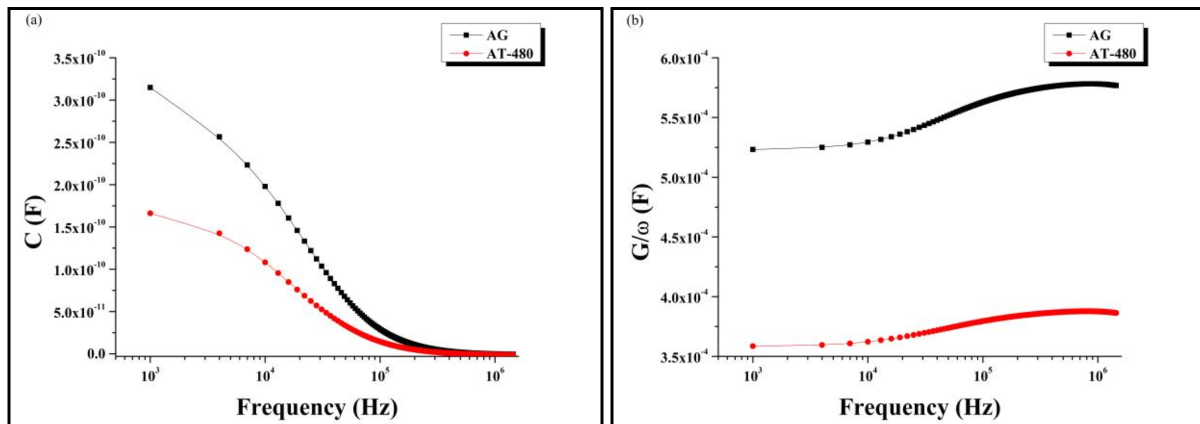

***Figure 5. a)** Capacitance-Frequency and **b)** Conductance-Frequency Measurements of AG and AT-480 V_2O_5 Thin Films*

3.3.3. Dielectric

The complex dielectric permittivity (ε^*) can be written as (Karaduman Er et al., 2021);

$$\varepsilon^* = \varepsilon' + i\varepsilon''$$

where $\varepsilon' = \frac{C}{C_0}$ is the real part that is known as dielectric constant and $\varepsilon'' = \frac{G}{\omega C_0}$ is the imaginary part that is known as dielectric loss. $\omega = 2\pi f$ is the angular frequency of electric field, $C_0 = \varepsilon_0 \frac{A}{d}$ is capacitance of free space, A is area and d is thickness of the films, ε_0 is permittivity of free space, C and G are respectively the measured capacitance and conductance. The frequency dependence of dielectric properties at room temperature for the AG and AT-480 thin films is calculated and plotted in Figure 6.

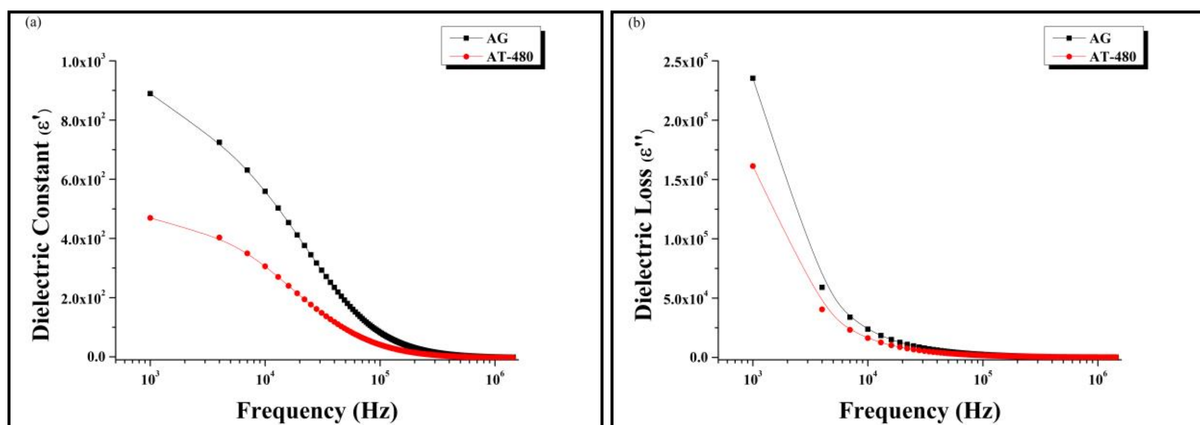

***Figure 6.** The Frequency-Dependent Behavior of **a)** Dielectric Constant and **b)** Dielectric Loss of AG and AT-480 V_2O_5 Thin Films*

Figure 6a shows the dielectric constant of AG and AT-480 samples at room temperature. As frequency increased, the dielectric constant of both samples was found to decrease. The dielectric constant is observed to decrease with increasing frequency due to the inability of induced dipoles to arrange themselves in the direction of the applied field (Sengodan et al., 2013). A similar situation was also reported earlier in the literature by Thomas & Jayalekshmi (1989). Furthermore, with the post-annealing process, the dielectric constant of the AT-480 film decreased. Similar results have been reported by Ahmed et al. (2019). Subsequently, an increase in the annealing temperatures caused a further decrease in the dielectric constant as was demonstrated earlier in the literature (Arshad et al., 2014). The significant changes in the dielectric constant after the post-annealing process may be due to phase change caused by annealing (Obstarczyk et al., 2019).

Figure 6b shows the dielectric loss of AG and AT-480 samples at room temperature. It is clear from the figure that the dielectric loss of both samples decreased as the frequency is increased. The observed decrease in dielectric loss can be ~~also~~ related to the aspects of electrical polarization. At low frequencies, the dipoles contribute to the polarization since they can orient themselves with the electric field. However, as frequency increases, the dipole response becomes limited and thus the dielectric loss becomes low as well (Kumar et al., 2016). Besides that, the AG sample recorded higher dielectric loss values than that of AT-480 only in the low frequency region (up to about 10^4 Hz), beyond which both samples had approximately same loss values.

4. CONCLUSION

In summary, the effect of post-annealing treatment on structural, morphological, optical and electrical properties of DC reactive magnetron sputtered amorphous V_2O_5 films grown on microscope glass slides has been thoroughly examined by XRD, SEM, UV-Vis as well as I-V and C-V electric measurements, respectively. Structural studies revealed that the post-annealing treatment improves the crystal quality of an originally amorph structure. Surface morphologies of the films changed from amorphous flat-like structure to V_2O_5 nanorods structure accompanied with an increase in roughness and grain size of the films under the effect of post-annealing treatment. The optical band gap energy recorded a remarkable decrease from 3.28 eV to 2.32 eV with the post-annealing treatment. Besides that, the changes in phase and morphology caused by post-annealing treatment have also induced some considerable changes in electric and dielectric properties of the films. The 480°C post-annealed film exhibited higher electric resistance (2720 Ω) compared to the unannealed film (1878.5 Ω) at room temperature. The increase in resistance was associated with a decrease in capacitance and dielectric constant. Nonetheless, the steep decrease of dielectric loss as compared to the slight decrease in dielectric constant with frequency demonstrates the eligibility of both materials for the manufacture of devices operating at mid-frequencies (particularly in the range of 10 kHz where dielectric losses are small enough compared to dielectric constant values).

ACKNOWLEDGEMENT

Authors would like to thank to Dr. Mustafa YILDIRIM and Emrah DIRICAN for their valuable supports and for their assistance during thin film deposition at METU MEMS Center. Authors also thank to Ahmad AJJAQ and Tayfun AGIR for the fruitful discussion on manuscript.

CONFLICT OF INTEREST

The authors declare no conflict of interest.

REFERENCES

Ahmed, N. M., Sabah, F. A., Abdulgafour, H. I., Alsadig, A., Sulieman, A., & Alkhoaryef, M. (2019). The effect of post annealing temperature on grain size of indium-tin-oxide for optical and electrical properties improvement. *Results in Physics*, *13*, 102159. doi:10.1016/j.rinp.2019.102159

Ba, C., Bah, S. T., D'Auteuil, M., Ashrit, P. V., & Vallée, R. (2013). Fabrication of high-quality VO2 thin films by ion-assisted dual ac magnetron sputtering. *ACS Applied Materials and Interfaces*, *5*(23), 12520-12525. doi:10.1021/am403807u

Benmoussa, M., Outzourhit, A., Bennouna, A., & Ameziane, E. L. (2002). Electrochromism in sputtered V2O5 thin films: Structural and optical studies. *Thin Solid Films*, *405(1–2)*, 11–16. https://doi.org/10.1016/S0040-6090(01)01734-5

Béteille, F., & Livage, J. (1998). Optical Switching in VO_2 Thin Films. *Journal of Sol-Gel Science and Technology*, *13*(1-3), 915-921. doi:10.1023/a:1008679408509

Bowman, R. M., & Gregg, J. M. (1998). VO_2 thin films: Growth and the effect of applied strain on their resistance. *Journal of Materials Science: Materials in Electronics*, *9*(3), 187-191. doi:10.1023/A:1008822023407

Budaguan, B. G., Sherchenkov, A. A., Chernomordic, V. D., Biriukov, A. V., & Ljungberg, L. Y. (1998). A-Si:H/c-Si heterostructures prepared by 55 kHz glow discharge high-rate deposition technique. *Journal of Non-Crystalline Solids*, *227-230*, *Part 2*, 1123-1126. doi:10.1016/S0022-3093(98)00289-0

Cho, C-R., Cho, S., Vadim, S., Jung, R., & Yoo, I. (2006). Current-induced metal-insulator transition in VOx thin film prepared by rapid-thermal-annealing. *Thin Solid Films*, *495*(1-2), 375-379. doi:10.1016/j.tsf.2005.08.241

Hébert, C., Willinger, M., Su, D. S., Pongratz, P., Schattschneider, P., & Schlögl, R. (2002). Oxygen K-edge in vanadium oxides: Simulations and experiments. *The European Physical Journal B - Condensed Matter and Complex Systems*, *28*(4), 407-414. doi:10.1140/epjb/e2002-00244-4

Hu, Y., Diao, X., Wang, C., Hao, W., & Wang, T. (2004). Effects of heat treatment on properties of ITO films prepared by rf magnetron sputtering. *Vacuum*, *75*(2), 183-188. doi:10.1016/j.vacuum.2004.01.081

Karaduman Er, I., Çağırtekin, A. O., Artuç, M., & Acar, S. (2021). Synthesis of Al/HfO2/p-Si Schottky diodes and the investigation of their electrical and dielectric properties. *Journal of Materials Science: Materials in Electronics*, *32*(2), 1677–1690. doi:10.1007/s10854-020-04937-9

Kim, H. K., You, H., Chiarello, R. P., Chang, H. L. M., Zhang, T. J., & Lam, D. J. (1993). Finite-size effect on the first-order metal-insulator transition in VO_2 films grown by metal-organic chemical-vapor deposition. *Physical Review B*, *47*(19), 12900-12907. doi:10.1103/PhysRevB.47.12900

Kiri, P., Warwick, M. E. A., Ridley, I., & Binions, R. (2011). Fluorine doped vanadium dioxide thin films for smart windows. *Thin Solid Films*, *520*(4), 1363-1366. doi:10.1016/j.tsf.2011.01.401

Kumar, R. T. R., Karunagaran, B., Mangalaraj, D., Narayandass, S. K., Manoravi, P., & Joseph, M. (2004). Characteristics of amorphous VO_2 thin films prepared by pulsed laser deposition. *Journal of Materials Science*, *39*(8), 2869-2871. doi:10.1023/B:JMSC.0000021467.53474.e3

Kumar, N. S., Raman, M. S., Chandrasekaran, J., Priya, R., Chavali, M., & Suresh, R. (2016). Effect of post-growth annealing on the structural, optical and electrical properties of V_2O_5 nanorods and its fabrication, characterization of V_2O_5/p-Si junction diode. *Materials Science in Semiconductor Processing*, *41*, 497-507. doi:10.1016/j.mssp.2015.08.020

Lamsal, C., & Ravindra, N. M. (2013). Optical properties of vanadium oxides-an analysis. *Journal of Materials Science*, *48*(18), 6341-6351. doi:10.1007/s10853-013-7433-3

Luo, Z., Zhou, X., Yan, D., Wang, D., Li, Z., Yang, C., & Jiang, Y. (2014). Effects of thickness on the nanocrystalline structure and semiconductor-metal transition characteristics of vanadium dioxide thin films. *Thin Solid Films*, *550*, 227-232. doi:10.1016/j.tsf.2013.10.172

Mohamed, H. A. (2007). The effect of annealing and ZnO dopant on the optoelectronic properties of ITO thin films. *Journal of Physics D: Applied Physics*, *40*(14), 4234-4240. doi:10.1088/0022-3727/40/14/019

Mohamed, H. A. (2009). Sintering process and annealing effect on some physical properties of V_2O_5 thin films. *Optoelectronics and Advanced Materials - Rapid Communications*, *3*(7), 693-699.

Obstarczyk, A., Kaczmarek, D., Mazur, M., Wojcieszak, D., Domaradzki, J., Kotwica, T., & Morgiel, J. (2019). The effect of post-process annealing on optical and electrical properties of mixed HfO_2–TiO_2 thin film coatings. *Journal of Materials Science: Materials in Electronics*, *30*(7), 6358-6369. doi:10.1007/s10854-019-00938-5

Prześniak-Welenc, M., Łapiński, M., Lewandowski, T., Kościelska, B., Wicikowski, L., & Sadowski, W. (2015). The Influence of Thermal Conditions on V_2O_5 Nanostructures Prepared by Sol-Gel Method. *Journal of Nanomaterials*, *2015*(Special Issue), 418024. doi:10.1155/2015/418024

Rajendra Kumar, R. T., Karunagaran, B., Senthil Kumar, V., Jeyachandran, Y. L., Mangalaraj, D., & Narayandass, S. K. (2003). Structural properties of V2O5 thin films prepared by vacuum evaporation. *Materials Science in Semiconductor Processing, 6(5–6)*, 543–546. doi: 10.1016/j.mssp.2003.08.017

Ramana, C. V., Smith, R. J., Hussain, O. M., & Julien, C. M. (2004). On the growth mechanism of pulsed-laser deposited vanadium oxide thin films. *Materials Science and Engineering B*, *111*(2-3), 218-225. doi:10.1016/j.mseb.2004.04.017

Sengodan, R., Shekar, B. C., & Sathish, S. (2013). Morphology, structural and dielectric properties of vacuum evaporated V_2O_5 thin films. *Physics Procedia*, *49*, 158-165. doi:10.1016/j.phpro.2013.10.022

Shimizu, K., Chinzei, I., Nishiyama, H., Kakimoto, S., Sugaya, S., Matsutani, W., & Satsuma, A. (2009). Doped-vanadium oxides as sensing materials for high temperature operative selective ammonia gas sensors. *Sensors and Actuators B: Chemical*, *141*(2), 410-416. doi:10.1016/j.snb.2009.06.048

Thomas, B., & Jayalekshmi, S. (1989). Dielectric properties of vanadium pentoxide thin films in the audiofrequency range. *Journal of Non-Crystalline Solids*, *113*(1), 65-72. doi:10.1016/0022-3093(89)90319-0

Van de Kerckhove, K., Mattelaer, F., Dendooven, J., & Detavernier, C. (2017). Molecular layer deposition of "vanadicone", a vanadium-based hybrid material, as an electrode for lithium-ion batteries. *Dalton Transactions*, *46*(14), 4542-4553. doi:10.1039/c7dt00374a

Vasanth Raj, D., Ponpandian, N., Mangalaraj, D., & Viswanathan, C. (2013). Effect of annealing and electrochemical properties of sol-gel dip coated nanocrystalline V_2O_5 thin films. *Materials Science in Semiconductor Processing*, *16*(2), 256-262. doi:10.1016/j.mssp.2012.11.001

Wang, N., Magdassi, S., Mandler, D., & Long, Y. (2013). Simple sol-gel process and one-step annealing of vanadium dioxide thin films: Synthesis and thermochromic properties. *Thin Solid Films*, *534*, 594-598. doi:10.1016/j.tsf.2013.01.074

Xue-Jin, W., Chun-Jun, L., Kang-Ping, G., De-Hua, L., Yu-Xin, N., Shi-Oiu, Z., Feng, H., Wei-Wei Z., & Zheng-Wei, C. (2008). Surface oxidation of vanadium dioxide films prepared by radio frequency magnetron sputtering. *Chinese Physics B*, *17*(9), 3512-3515. doi:10.1088/1674-1056/17/9/062

Vijayakumar, Y., Sayanna, R., Ramana Reddy, M. V. (2014). Annealing Effect on Structural, Optical and Electrical Properties of V_2O_5 Thin Films by Dip Coating. *Asian Journal of Applied Sciences*, *7*(8) 753-760. doi:10.3923/ajaps.2014.753.760

Yan, W., Hu, M., Wang, D., & Li, C. (2015). Room temperature gas sensing properties of porous silicon/V_2O_5 nanorods composite. *Applied Surface Science*, *346*, 216-222. doi:10.1016/j.apsusc.2015.01.020

Yelsani, V., Pothukanuri, N., Sontu, U. B., Yaragani, V., & Musku Venkata, R. R. (2019). Effect of annealing temperature on structural, morphological, optical and electrical properties of spray deposited V_2O_5 thin films. *Materials Science (Medžiagotyra)*, *25*(1), 3-6. doi:10.5755/j01.ms.25.1.18492

Zou, C. W., Yan, X. D., Han, J., Chen, R. Q., & Gao, W. (2009). Microstructures and optical properties of β-V_2O_5 nanorods prepared by magnetron sputtering. *Journal of Physics D: Applied Physics*, *42*(14), 145402. doi:10.1088/0022-3727/42/14/145402

Zou, C. W., Yan, X. D., Patterson, D. A., Emanuelsson, E. A. C., Bian, J. M., & Gao, W. (2010). Temperature sensitive crystallization of V_2O_5: from amorphous film to β-V_2O_5 nanorods. *CrystEngComm*, *12*(3), 691-693. doi:10.1039/b916614a